

A physical model for radiative, convective dusty disk in AGN.

A. Dorodnitsyn^{1,2,3}, T. Kallman¹

Abstract

An accretion disk in an Active Galactic Nucleus (AGN) harbors and shields dust from external illumination: at the mid-plane of the disk around a $M_{\text{BH}} = 10^7 M_{\odot}$ black hole, dust can exist at 0.1pc from the black hole, compared to 0.5pc outside of the disk. We construct a physical model of a disk region approximately located between the radius of dust sublimation at the disk mid-plane and the radius at which dust sublimates at the disk surface. Our main conclusion is that for a wide range of model parameters such as local accretion rate and/or opacity, the accretion disk's own radiation pressure on dust significantly influences its vertical structure. In addition to being highly convective, such a disk can transform from geometrically thin to slim. Our model fits into the narrative of a "failed wind" scenario of Czerny & Hryniewicz (2011) and the "compact torus" model of Baskin & Laor (2018), incorporating them as variations of the radiative dusty disk model.

1. Introduction

The radiative output of Active Galactic Nuclei (AGN) is powered by accretion of gas and most of the gas potential energy is released in the inner part of an accretion disk. However,

¹Laboratory for High Energy Astrophysics, NASA Goddard Space Flight Center, Code 662, Greenbelt, MD, 20771, USA

²University of Maryland, Baltimore County (UMBC/CRESST), Baltimore, MD 21250, USA

³Space Research Institute, 84/32, Profsoyuznaya st., Moscow, Russia

several crucial observational characteristics of AGN are shaped considerably further away, at $\text{few} \times 0.01 - 0.5 \text{ pc}$ from the Super-Massive Black Hole (BH). It is also at approximately this distance from the BH the radiation flux is sufficiently diluted such that dust grains can survive the illumination from the nucleus. The presence of dust results in a 10 – 100 -fold increase of opacity compared with only gas, which leads to a dramatic increase of coupling between the radiation from the nucleus and gas.

The radius outside of which dust can survive forms a dust sublimation surface, a boundary between the inner, mostly dust-free region and the outer part often associated with the dusty torus. The latter is invoked to explain the dichotomy between two types of AGN, in which optically thick equatorial material blocks the direct view onto the broad line region and the accretion disk in type 2 galaxies (Rowan-Robinson 1977; Antonucci 1984; Antonucci & Miller 1985; Urry & Padovani 1995).

Mid-infrared (MIR) interferometric observations of nearby AGN clearly point to the presence of dust (Jaffe et al. 2004; Raban et al. 2009; Tristram et al. 2014; Tristram & Schartmann 2011) at distances $\geq 0.1 \text{ pc}$ from the center. The relative numbers of type 1 and type 2 objects suggest that the obscuring material is geometrically thick.

The virial theorem predicts that in order to be geometrically thick at a distance, $r \simeq 1 \text{ pc}$, temperature of the obscuring gas should be of the order of 10^6 K for a $10^7 M_{\odot}$ BH. This is not compatible with survival of dust in the obscurer, and hence is in conflict with the presence of dust inferred from IR observations. On the other hand, the temperature expected at the surface of a thin accretion disk is $\leq 1000 \text{ K}$ at $\sim 1 \text{ pc}$ from the center.

Reverberation mapping (i.e. Koshida et al. 2014) is generally consistent with putting the inner boundary of the torus to within the dust sublimation surface at $0.4 - 0.5 \text{ pc}$ (Kaspi et al. 2000). The location of the broad line region (BLR) relative to the center has been measured by reverberation to be $\sim \text{few} \times 0.01 \text{ pc}$ (e.g. Peterson et al. 2004; Suganuma et al.

2006).

Magnetic or/and radiation driving have been proposed as a mechanisms behind the formation of the BLR and the torus. A line driven wind, i.e. a wind driven by the radiation pressure in UV lines (Proga & Kallman 2004; Murray et al. 2005), has a launching radius which is $\sim 10x$ smaller, and correspondingly characteristic line widths which are a factor $\sim 10x$ greater than indicated by the maximum BLR line widths. A line driven wind from an accretion disk is not massive enough to be the torus.

Magnetic fields, specifically large-scale magnetic fields, are an alternative or augmenting mechanism which can be the driving engine of the BLR and the torus. Semi-analytical or numerical models (Lovelace et al. 1998; Dorodnitsyn et al. 2016) show that large-scale B-field can support an AGN torus. Self-consistent numerical simulations of a thin disk threaded by the net vertical magnetic flux (Zhu & Stone 2018) show that thin disks cannot both transport large-scale magnetic fields (Lubow et al. 1994; Bisnovatyi-Kogan & Lovelace 2000, 2007) *and* simultaneously have a massive, polar, MHD-driven (Magneto-hydrodynamic) outflow. In addition, typical MHD flows have an approximate equipartition between magnetic energy density and gas energy. So the characteristic temperature of the gas near the launching radius of the magnetically-driven, gravitationally unbound outflow is also expected be of the order of the virial temperature.

Czerny & Hryniewicz (2011)(hereafter CH11) suggested that the disk’s own radiation may produce sufficient radiation pressure on dust grains that would expel a failed wind from the outer accretion disk atmosphere. Such a failed wind then would be responsible for the formation of the broad line region seen in Seyfert I galaxies. Developing this idea further, Baskin & Laor (2018) (BL18) concluded that the contribution from large graphite grains near $T \simeq 2000\text{K}$ increases dust opacity which results in a an inflated compact, torus-like structure near the observed BLR radius.

In a simple case, when dust is arranged in a spherically-symmetric shell it cannot survive closer than dust sublimation radius: $R_{\text{sub}} \simeq 0.2 - 0.5$ pc from a supermassive black hole. If dust is contained in a cold and dense accretion disk it can survive much closer to the BH, down to $\sim 10^{-3} - 10^{-2}$ pc (BL18, CH11). The radial scaling of the effective surface temperature of the disk: $T_{\text{eff}} \propto R^{-3/4}$ guarantees that beyond a certain radius, R_{din} , T drops below the dust sublimation temperature allowing survival of dust. This corresponds to a dramatic increase of the opacity. The disk radiation flux may be strong enough to produce a non-negligible radiation pressure $\propto (F/c)\kappa_d$, where κ_d is dust opacity. As suggested by CH11 and BL18 this can lead to the formation of failed winds or produce a "compact torus" at $\text{few} \times 10^{-2}\text{pc}$.

Previous work has demonstrated the likely importance of dust in the dynamics of the gas in the torus and BLR. However, there has not been an examination of the effects of dust on the internal structure of the accretion disk in the pc-scale region of AGN. The goal of this paper is to explore how radiation pressure on dust grains defines the vertical structure of the disk in the region where its temperature is comparable to dust sublimation temperature, T_{sub} . We will show that such changes are important, and lead to verifiable results. A preview of the results is as follows:

- We first will develop an analytical model of an accretion disk, based on a modified α disk approach, that includes contributions from gas pressure and radiation pressure on dust. We show that there is a difference between the radius of dust sublimation at the disk mid-plane and the radius at which dust sublimates at the disk surface.
- There is a region in the AGN accretion disk where the radiation pressure from the disk's own near- and mid-infrared radiation shapes the vertical disk structure. In this paper we call this part of the disk the "Active Dusty Region" (ADR).
- It is well known that radiation pressure often leads to a strong convective instability

both in stellar envelopes and in radiative disks. Developing a semi-analytical disk model, we calculate the parameter range where convection develops due to vertical radiation pressure on dust and calculate the disk properties.

- The internal radiation push can provide an explanation of the geometrically thick obscuration and avoids the apparent paradoxes associated with gas pressure or turbulent vertical support. The main parameter which determines the importance of local radiation pressure is the local accretion rate \dot{M}_{loc} . The disk becomes locally geometrically thick if the accretion is locally super-Eddington, with the latter calculated with dust opacity which is 10-100 times larger than the typical opacity of gas without dust. The latter allows to make an argument that the obscuration associated with type-2 AGN can be attributed to a super-critical dusty accretion in the ADR region, calculated in this paper.

The structure of this paper is as follows. In Section 2 we begin to examine the effects of the disk’s own radiation pressure on dust on the disk vertical structure. In Section 3 we further derive properties of the Active Disk Region. In Section 4 we calculate a detailed analytical and numerical solution of the disk equations and in Section 5 we show that in a wide range of parameters the radiative dusty disk is convectively unstable. The results are summarized in Section 7 along with the limitations of our approach, and the ideas developed in this paper are put in the context of the broader AGN accretion disk physics. We conclude with Section 8.

2. Properties of AGN at pc-scales

In this section we examine the effect of dust formation or survival and its dependence on the global parameters of the AGN. In doing so, we adopt standard assumptions about

accretion in a thin disk around a BH (Shakura & Sunyaev 1973; Lynden-Bell & Pringle 1974).

2.1. Global parameters

It is customary to express the total luminosity of the AGN in terms of the accretion rate:

$$L = \epsilon \dot{M} c^2, \quad (1)$$

which is equivalent to the definition of an accretion efficiency, ϵ - a parameter that is approximately bounded between 0.057 for a non-rotating BH and 0.42 for a BH rotating at maximum efficiency. The mass-accretion rate, \dot{M} in (1) corresponds to the innermost part of the disk where the most of the radiative output is produced. After assuming ϵ , it is standard to equate (1) to the Eddington luminosity:

$$L_E = \frac{4\pi cGM}{\kappa_e} = 1.25 \times 10^{45} M_7 \text{ erg s}^{-1}, \quad (2)$$

where M is the mass of the BH, and to scale accretion rate in terms of “Eddington” accretion rate:

$$\dot{M}_E \simeq 0.22 \epsilon_{0.1}^{-1} M_7 M_\odot \text{ yr}^{-1}, \quad (3)$$

where in (2) and (3) the following parameters are adopted: $\kappa_e = 0.4 \text{ cm}^2 \text{ g}^{-1}$ is the Thomson opacity; we scale the BH mass in units of $M_7 = M/10^7 M_\odot$ and fix the efficiency of accretion $\epsilon = 0.1$.

The above picture is augmented with the assumption that enough medium is supplied to the AGN from galactic scales near the AGN outer radius, R_{AGN} . It is customary to define this as a radius where the gravity from the BH dominates the gravitational field of the host galaxy:

$$R_{\text{AGN}} = \frac{GM}{\sigma_{\text{Blg}}^2} \simeq 4.30 M_7 \left(\frac{\sigma_{\text{Blg}}(\text{kms}^{-1})}{100} \right)^{-2} \text{pc} = 4.5 \times 10^6 \left(\frac{\sigma_{\text{Blg}}(\text{kms}^{-1})}{100} \right)^{-2} R_g, \quad (4)$$

where σ_{Blg} is the stellar velocity dispersion in the bulge, and the last equality is given in terms of the Schwarzschild gravitational radius of the BH:

$$R_g = \frac{2GM}{c^2} = 2.95 \times 10^{12} M_7 \text{cm}. \quad (5)$$

Hereafter, we reserve R for the radius in physical units, and r for the scaled radius: $r_y = R/y$.

A crude estimate for the vertical scale height of the disk at R_{AGN} is done assuming the scaling for the disk height: $H \sim v_{\text{T}}/\Omega$, where H is the half-thickness of the disk, $\Omega = (GM/R^3)^{1/2}$ is the orbital velocity and v_{T} is the isothermal sound speed, $v_{\text{T}} = (\mathcal{R}_{\text{gas}}T/\mu_m)^{1/2}$, and μ_m is the mean molecular weight and \mathcal{R}_{gas} is the gas constant. Hereafter while calculating disk properties we neglect the disk self-gravity, and from equation (6) it follows that at R_{AGN} the disk is very thin:

$$H/R_{\text{AGN}} \simeq 6.45 \times 10^{-3} \sigma_{\text{Blg},100}^{-1} T_{50}^{1/2}. \quad (6)$$

Consequently, such a disk intercepts only a small fraction of the radiation flux from the nucleus.

It is instructive to review the radiative energy density generated locally in the disk and compare it to that from external illumination. Radiation flux at pc-scales is dominated by

the flux from the nucleus, F_{ext} which is produced in the inner parts of the disk. Its angular dependence is the manifestation of the limb darkening effect in the disk, and has a simple dependence on $\mu = \cos \theta$ where θ is the inclination angle from the normal to the disk (i.e. Sobolev 1975; Sunyaev & Titarchuk 1985):

$$F_{\text{ext}} \simeq 6 \times 10^9 f(\theta) \dot{M}_{0.1} \epsilon_{0.1} r_{0.1}^{-2} \text{ erg cm}^{-2} \text{ s}^{-1} \gg F_{\text{loc}} \quad (7)$$

where $f(\theta) = \mu(2\mu + 1)$ is the angular dependence of the radiation flux. The local radiation flux generated in the disk, i.e. the normal flux at the disk's photosphere reads

$$F_{\text{loc}} = \frac{3}{8\pi} \frac{GM}{r^3} \dot{M}_{\text{loc}} \simeq 3.4 \times 10^4 r_{0.1}^{-3} \dot{M}_{\text{loc},0.1} M_7 \text{ erg} \cdot \text{cm}^{-2} \cdot \text{s}^{-1}, \quad (8)$$

and it follows that until matter can spiral down to a fraction of a parsec, the release of the gravitational potential energy produces local radiative output that is negligible for the gas dynamics. Radiation flux, F_{ext} depends on the mass-accretion rate in the inner disk, while F_{loc} depends on local accretion rate, and in the following we reserve \dot{M} for global, and \dot{M}_{loc} for local accretion rates.

If a thin, cold, dusty disk is illuminated by the UV flux F_{ext} , due to very high UV opacity the radiation is stopped immediately near the surface of the disk heating dust to approximately T_{sub} . Assuming all incoming radiation is converted to IR it follows that the temperature in such an idealized cold disk is *decreasing* towards the equatorial plane. The vertical component of radiation pressure, $\mathbf{g}_{z,\text{rad}} \propto (\nabla T)_z$ then points downwards and is balanced by the vertical gradient of the gas pressure at the characteristic density:

$$n_{\text{eq}} = n(P_g = P_r) \simeq 6.12 \times 10^{10} T_{1500}^3 \text{ cm}^{-3}, \quad (9)$$

where T_{1500} is the dust temperature scaled in units of $T_{\text{sub}} = 1500\text{K}$, also P_g is the gas

pressure:

$$P_g = \rho \mathcal{R} T, \quad (10)$$

and P_r is the radiation pressure:

$$P_r = aT^4/3, \quad (11)$$

where a is the radiation constant, and to simplify notation such as in (10), the mean molecular weight, μ_m is absorbed in the definition of the gas constant, $\mathcal{R} = \mathcal{R}_{\text{gas}}/\mu_m$, and in the rest of the paper we adopt $\mu_m = 1$ (see also Glossary). Even when radiation pressure on dust is important in the bulk of the disk, at mid-plane the density exceeds the density in equation 9, $n_c \gg n_{\text{eq}}$, so despite the enhanced opacity due to dust the mid-plane pressure is dominated by P_g .

Accretion in a thin disk far from a BH is slow. The free-fall time-scale is the shortest in the hierarchy of time-scales: $t_{\text{dyn}} = 1.49 \times 10^2 r_{0.1}^{3/2} \text{yr}$. However, the accretion time-scale corresponds to the viscous time-scale t_{visc} in the disk:

$$t_a \propto t_{\text{visc}} = \frac{R}{v_r} = 5.15 \times 10^7 r_{0.1}^{1/2} T_{1500}^{-1} \alpha_{0.1}^{-1} \text{yr}, \quad (12)$$

where $\alpha < 1$ is the effective viscosity parameter, introduced by Shakura (1972), and $\alpha_{0.1} = \alpha/0.1$. A geometrically thin disk cools efficiently through radiative losses and as the disk cooling-time is much smaller than t_a : $t_{\text{th}} = 1/(\alpha \Omega) = 1.492 \times 10^3 \alpha_{0.1}^{-1} r_{0.1}^{3/2} \text{yr}$, it is approximately $t_{\text{dyn}} \lesssim t_{\text{th}}$.

From (12) it is clear that a buildup of matter (in a thin disk) at large radii cannot quickly propagate through the disk towards smaller radii. Hence we allow the situation in which the local accretion rate exceeds the rate at the center, $\dot{M}_{\text{loc}} \neq \dot{M}$. The role of the

local accretion rate \dot{M}_{loc} is to define the local rate of energy production in the disk, and correspondingly the local vertical radiation flux, F_{loc} in (8).

2.2. Disk thickness When Radiation Pressure is Important

Assuming a thin disk approximation the equation for vertical balance reads:

$$\frac{dP_g}{dz} = -\rho g_z + \rho \frac{F_{\text{loc}} \kappa}{c}, \quad (13)$$

where κ is the opacity of the accreting material which is assumed to be comparable to that of dust, κ_d . The vertical gravitational acceleration, g_z is found from:

$$g_z = \Omega^2 z. \quad (14)$$

The disk, throughout this paper, is assumed to be Keplerian, $\Omega = \Omega_K$, where

$$\Omega_K = (GM R^{-3})^{1/2}. \quad (15)$$

In the case when radiation pressure dominates, the characteristic scale-height of the disk follows from (13) after neglecting the contribution from the gas pressure:

$$H/R \simeq \frac{3}{2} \frac{\dot{M}_{\text{loc}}}{\dot{M}_{\text{loc,cr}}} \simeq 8 \times 10^{-3} \kappa_{10} \dot{M}_{\text{loc},0.1} r_{0.01}^{-1}, \quad (16)$$

where $\dot{M}_{\text{loc,cr}}$ is the Eddington accretion rate, calculated using dust opacity κ_d .

$$\dot{M}_{\text{loc,cr}} = \frac{4\pi cr}{\kappa_d} \simeq 12.3 \kappa_{10}^{-1} r_{0.01} M_{\odot} \text{yr}^{-1}, \quad (17)$$

where $\kappa_x = \kappa/x$ is the opacity scaled in $x(\text{cm}^2 \text{g}^{-1})$ units of opacity, and $\dot{M}_{\text{loc},0.1}$ is the local accretion rate scaled in $0.1M_{\odot}\text{yr}^{-1}$. In a model of the dust opacity which takes into account the contribution from large graphite grains (BL18) the critical mass-accretion rate would be correspondingly smaller: $\dot{M}_{\text{loc,cr}} = 2.5 \kappa_{50}^{-1} M_{\odot}\text{yr}^{-1}$. If the local accretion rate exceeds $\dot{M}_{\text{loc,cr}}$ then the disk scale height becomes comparable to the radius. For the same set of parameters the critical value of \dot{M} calculated assuming only electron scattering opacity is $\dot{M}_{\text{E}} \simeq 0.2M_{\odot}\text{yr}^{-1}$. For the disk not to be super-Eddington globally, the excess mass of the gas $\sim \text{few } M_{\odot}\text{yr}^{-1}$ should be expelled via winds along the way towards the BH.

One can notice that the gas density in the disk mid-plane is much higher than required by (9), so when internal radiation pressure of the disk is negligible the gas pressure from the disk can balance radiation pressure due to external radiation at plausible levels. If the thick disk is supported by the radiation pressure, the condition $H/R \propto 1$ can be recast as a consequence of the Virial theorem for the disk temperature, namely $T \simeq T_{\text{vir,r}}$ where $T_{\text{vir,r}}$ is the “virial” temperature for the radiation dominated medium (Dorodnitsyn et al. 2011):

$$T_{\text{vir,r}} = \left(\frac{GM}{aR} \right)^{1/4} \simeq 1755.93 \left(\frac{M_7(n/10^7)}{r_{0.1}} \right)^{1/4} \text{ K}, \quad (18)$$

derived for a spherically symmetric shell.

3. Dust Sublimation Region in a Disk

3.1. The Inner and Outer Dust Sublimation Scales

In order to calculate the structure of a thin disk, the assumption was made in (SS73) that viscous dissipation is proportional to the gas density ρ . Here we assume that all the dissipated energy is transported vertically by radiation. This gives the following estimate

for the temperature at the disk surface:

$$T_s = 879 \left(\frac{M_7 \dot{M}_{\text{loc},0.1}}{r_{0.01}^3} \right)^{1/4} \text{ K} \quad (19)$$

where it was assumed that $T_s = T(\tau_{\text{phot}} = 2/3)$ in which τ_{phot} is the optical depth at the disk photosphere. When $R = 10^{-3}\text{pc}$ the surface temperature reaches 1479K and little dust can survive in the disk.

If external illumination is neglected, the vertical decrease of temperature within a disk ensures that the mid-plane temperature, T_c is always greater than the surface temperature T_s . Approximately, T_c is a factor of $\tau_c^{1/4}$ greater than T_s , where τ_c is the vertical optical depth of the disk (see Section 4). In general τ_c should be calculated from the solution for the vertical structure of the disk. From standard gas pressure only α -disk solution we get

$$\begin{aligned} T_c &= \frac{1}{2} \left(\frac{3}{2} \right)^{1/5} \kappa^{1/5} J(R)^{2/5} \mu_m^{1/5} \dot{M}_{\text{loc}}^{2/5} \pi^{-2/5} \Omega^{3/5} \mathcal{R}^{-1/5} \alpha^{-1/5} \sigma_B^{-1/5} \\ &\simeq 2 \times 10^3 \kappa_{10}^{1/5} M_7^{3/10} \dot{M}_{\text{loc},0.1}^{2/5} r_{0.1}^{-9/10} \text{ K}, \end{aligned} \quad (20)$$

where the factor $J(R)$ is related to the inner boundary condition near the BH and for sub-parsec distances it is $J \simeq 1$ to a good accuracy, and $\sigma_B = ac/4$ is the Stefan-Boltzmann constant.

Figure 1 shows graphs of $T_s(R)$ from (19) and $T_c(R)$ from (20). Two intersections of these two curves with the T_{sub} line define the inner, R_{in} and outer, R_{out} dust sublimation radii in a disk. The inner sublimation radius is defined as the radius where the disk surface temperature equals dust sublimation temperature:

$$\begin{aligned}
 R_{\text{in}} &\simeq 5 \times 10^{-3} M_7^{1/3} \dot{M}_{\text{loc},0.1}^{1/3} T_{\text{sub},1500}^{-4/3} \text{PC} \\
 &\simeq 5 \times 10^3 M_7^{-2/3} \dot{M}_{\text{loc},0.1}^{1/3} T_{\text{sub},1500}^{-4/3} r_g.
 \end{aligned} \tag{21}$$

where $T_{\text{sub},1500}$ is the dust sublimation temperature in units of 1500K. Similarly, from (20), we define an outer sublimation radius, R_{out} as such a radius that at $R \leq R_{\text{out}}$ dust sublimates at the mid-plane:

$$\begin{aligned}
 R_{\text{out}} &\simeq 0.14 M_7^{1/3} \kappa_{10}^{2/9} \dot{M}_{\text{loc},0.1}^{4/9} \alpha_{0.1}^{-2/9} T_{\text{sub},1500}^{-10/9} \text{PC} \\
 &\simeq 1.5 \times 10^5 \dot{M}_{\text{loc},0.1}^{4/9} \kappa_{10}^{2/9} M_7^{-2/3} \alpha_{0.1}^{-2/9} T_{\text{sub},1500}^{-10/9} r_g.
 \end{aligned} \tag{22}$$

Since R_{out} is found from $T(\Sigma_c) = T_{\text{sub}}$, the disk's column density, $\Sigma_c = 2\rho_c H$ should be found from the solution for the disk.

As the gas spirals to $R \leq R_{\text{out}}$, T becomes greater than dust sublimation temperature T_{sub} . Dust is destroyed first near the mid-plane and then, as r gets smaller, progressively above. Naturally $R_{\text{out}} > R_{\text{in}}$ defining the region within the disk where hot dust exists at some height in the disk. Notice that at $R = R_{\text{out}}$ disk surface is quite cool: $T_s \simeq 156 \left(M_7 \dot{M}_{0.1} \right)^{1/4} r_{0.1}^{-3/4} \text{K}$. Such a difference between T_s and T_c is essentially the result of the blanketing effect from the disk. Dependence of R_{in} and R_{out} on M follows if we assume the scaling $\dot{M}_{\text{loc}} \propto \dot{M} \propto L_{\text{Edd}} \propto M$:

$$R_{\text{in}} \propto M^{2/3}, \tag{23}$$

and

$$R_{\text{out}} \propto M^{7/9}. \tag{24}$$

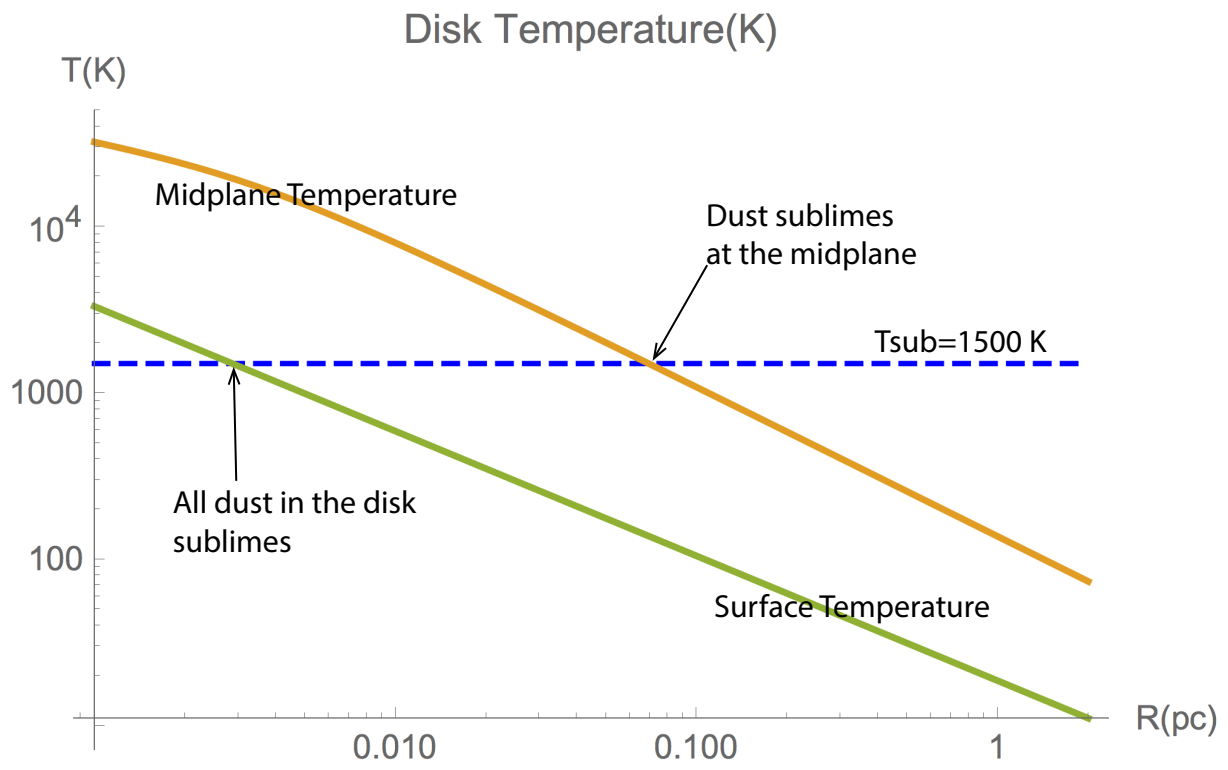


Fig. 1.— Schematics of the dusty region in a disk

Increasing the mass of the BH, we obtain $R_{\text{in}} \simeq 0.1\text{pc}$, and $R_{\text{out}} \simeq 5\text{pc}$ for $M = 10^9 M_{\odot}$.

The accretion rate near the BH, \dot{M} determines the central luminosity L through (1) and thus the global dust sublimation radius R_{sub} (see Section 3).

$$R_{\text{sub}} = 0.13 \left(\frac{f(\theta)\epsilon_{0.1}\dot{M}_{0.1}}{T_{1500}^4} \right)^{1/2} \text{pc}, \quad (25)$$

where $f(\theta) = \mu(2\mu + 1)$ is the angular dependence of the radiation flux from the nucleus, i.e. (63). The result is the dust sublimation surface, which, generally speaking, is different from a simple spherically symmetric case such as (25) which was calculated for $f = 1$. Notice that there is a difference between our definition of R_{out} in (22) and the definition of BL18. The latter define R_{out} as the dust sublimation radius for AGN (25) because their work studies the size of the BLR rather than the structure and properties of the disk itself. As long as energy is transported vertically via radiation, it follows from (22) and (21) that $R_{\text{out}} \propto \dot{M}_{\text{loc},0.1}^{1/9} R_{\text{in}}$. Another interesting scaling: $R_{\text{sub}}/R_{\text{out}} \sim (\dot{M}/\dot{M}_{\text{loc}})^{1/2}$ follows from (22), (25).

Without the shielding protection of the accretion disk the fate of dust above such disk depends on whether it is inside or outside the AGN dust sublimation surface $R_{\text{sub}}(\theta)$:

1. if $R_{\text{sub}} \gtrsim R_{\text{out}}$, the dust above the disk does not survive.
2. if $R_{\text{in}} \lesssim R_{\text{sub}} \lesssim R_{\text{out}}$, depending on \dot{M}_{loc} the disk can be 1) thin or 2)thick/outflowing, (the situation is illustrated in Figure 2).

When \dot{M}_{loc} exceeds

$$\dot{M}_{\text{loc}}(R_{\text{sub}} = R_{\text{out}}) = 0.08 \left(\frac{M_7^{1/3} T_{1500}^{8/9} \kappa_{10}^{2/9}}{\alpha_{0.1}^{2/9} \epsilon_{0.1}^{1/2}} \right)^{-9/4} \dot{M}_{0.1}^{9/8} M_{\odot} \text{yr}^{-1}, \quad (26)$$

the condition $R_{\text{sub}} \leq R_{\text{out}}$ is fulfilled, at least part of the active region above the disk is shielded beyond the AGN dust sublimation surface.

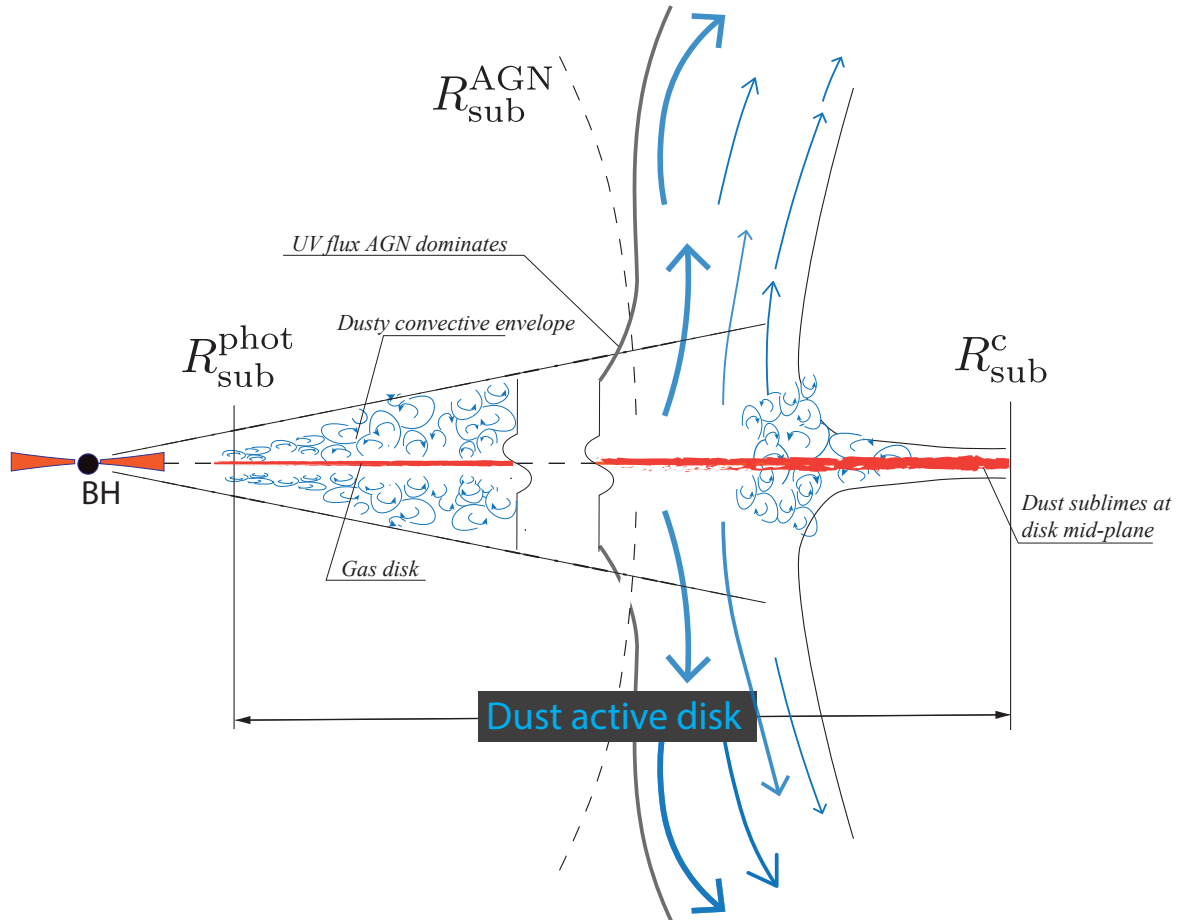


Fig. 2.— Convective dusty disk with an outflow. When $\dot{M}_{\text{loc}} \gtrsim \dot{M}(L_{\text{bol}})$ (i.e accretion is locally supercritical) disk’s own radiation pressure pushes dust above the disk. At $R > R_{\text{sub}}^{\text{AGN}}$ disk outflow is launched by the disk’s own IR pressure, with a possibility to being further accelerated by the radiation pressure from the nucleus. Not to scale.

4. Solution for the Disk Vertical Structure

4.1. Basic equations

In this section we describe the details of our model used to derive estimates in the previous sections. We adopt the α -disk theory of SS73 and include pressure of infrared (IR) radiation on dust in the disk interior. The radiation is produced by viscous dissipation and assumed to be in thermodynamic equilibrium with gas-dust mixture. Dust particles are assumed to be fully coupled to the gas.

The equation of state is that of a mixture of ideal gas and radiation:

$$P = P_g + P_r, \tag{27}$$

where P is the total pressure, P_r is the radiation pressure defined in (11), and P_g is the gas pressure defined in (10). Analytic solutions for the limiting cases of $P_g \ll P_r$, and $P_g \gg P_r$ are derived in (Shakura & Sunyaev 1973). Here we will solve the disk equations for arbitrary P_g and P_r assuming constant opacity.

We assume that in the ADR region, accretion proceeds near the equatorial plane:

$$\dot{M} = 2\pi r v \Sigma, \tag{28}$$

where to simplify notation in this section $\dot{M} = \dot{M}_{\text{loc}}$ is the time averaged accretion rate, v is the radial gas velocity and Σ is the surface density:

$$\Sigma = \int_{-H}^H \rho dz \simeq 2H \rho, \tag{29}$$

where H is the vertical scale-height of the disk and $\rho = \rho(z = 0)$, i.e. in a single-layer disk

model, all height-dependent quantities are taken at the disk mid-plane.

$$\nu\Sigma = \frac{1}{3\pi}\dot{M}, \quad (30)$$

where we neglected a factor, related to the inner boundary condition, (i.e. $J(R)$ in (20)).

The viscosity ν in (46) is proportional to the total pressure, P :

$$\nu = \alpha \frac{P}{\Omega\rho}. \quad (31)$$

The only relevant component of the radiation flux in a pc-scale thin disk is the vertical one.

The vertical flux F satisfies:

$$\frac{\partial F}{\partial z} = \frac{9}{4}\rho_c q_v \equiv \frac{9}{4}\Omega^2\rho_c\nu, \quad (32)$$

where $q_v(\text{ergs} \cdot \text{s}^{-1} \cdot \text{g}^{-1})$ is the specific rate of viscous energy dissipation:

$$q_v = \Omega^2\nu. \quad (33)$$

Integrating equation (32) between $-H$ and $+H$, one gets the vertical radiation flux from the disk surface:

$$F^+ = \frac{3}{8\pi}\dot{M}\Omega^2. \quad (34)$$

An implicit assumption was made when integrating (32) to obtain (34). That is, after equation (32) was rewritten as $\frac{\partial F}{\partial \sigma} = \frac{9}{4}q_v$, where

$$\sigma(z) = \int_0^z \rho dz, \quad (35)$$

is the mass coordinate, and then integrated over height, and it was assumed that the rate of *specific* viscous dissipation, q_v is constant.

The radiation moment equation in a plane-parallel case valid for the geometrically thin disk is:

$$\frac{\partial E}{\partial \tau} = 3 \frac{F}{c}, \quad (36)$$

where E and F are radiation energy density and radiation flux and τ is the vertical optical depth.

The boundary condition for (36) is $E(\tau = 0) = 2F^+/c$. Integrating (36) results in $E = (3F^+/c)(\tau + 2/3)$ and

$$\sigma_B T^4 = \frac{27}{64} \nu \kappa \Omega^2 \Sigma^2, \quad (37)$$

introducing the subscript "c" for mid-plane quantities, from (37) it follows that if $\tau_c \gg 1$, where $\tau_c = \int_0^H \kappa \rho dz \simeq \Sigma \kappa_d$ then (20) gives:

$$T_c \propto \tau_c^{1/4} T_s, \quad (38)$$

4.2. Solution with radiation pressure

The solution for T for gas-dominated disk was given in (20). As T approaches T_{sub} , the radiation pressure becomes important. When $T_c > T_{\text{sub}}$ a gas-only layer at the mid-plane is enveloped in a dusty-gaseous envelope above the mid-plane. From above its temperature is bound by $T^+ \lesssim T_{\text{sub}}$, and the transition from gas-dominated layer to dust-dominated envelope is happening at the height H_g . The estimate of scale-height H_g follows from (13):

$$\begin{aligned}
 H_g/R &\simeq \left(\frac{P_c - P^+}{\rho_c \Omega^2} \right)^{1/2} \lesssim \left(\frac{\mathcal{R}T_{\text{sub}}}{\Omega^2} \right)^{1/2} \\
 &\simeq 5.4 \times 10^{-3} (T_{1500} r_{0.1} / M_7)^{1/2},
 \end{aligned}
 \tag{39}$$

i.e. the gas layer is very geometrically thin.

It is beyond of the scope of this paper to calculate the vertical structure of the disk with the gas to dust transition. Instead, we adopt a single layer approximation with the temperature dependent opacity (see further (51)) Thus in the following our goal is to calculate the *average* properties of the disk which is supported by an arbitrary combination of gas and radiation pressure: $P = P_{\text{gas}} + aT^4/3$.

Assuming the relation:

$$\rho = \frac{\Sigma}{2H},
 \tag{40}$$

then the total pressure, P (reminding that the molecular weight is absorbed in the gas constant \mathcal{R}) is

$$P = \rho \left(\mathcal{R}T + \frac{2aT^4 H}{3\Sigma} \right).
 \tag{41}$$

The approximate relation for the scale-height follows from the equation for the vertical balance:

$$\frac{dP}{dz} = -\rho g_z,
 \tag{42}$$

which is equivalent to (13), after noticing that in diffusion approximation

$$F = -c/(\kappa\rho)dP_r/dz,
 \tag{43}$$

and thus recovering:

$$H^2 = \frac{P}{\Omega^2 \rho}. \quad (44)$$

Equation (44) is the equivalent of the vertical balance equation. Substituting (41) and (40) to (44) there follows a useful relation:

$$\Sigma = \frac{2aHT^4}{3(H^2\Omega^2 - \mathcal{R}T)}. \quad (45)$$

After substituting (41) and (40) to (31) there follows another relation:

$$\nu = \frac{\alpha(2aHT^4 + 3\mathcal{R}\Sigma T)}{3\Sigma\Omega}. \quad (46)$$

The third useful relation we can get from a system of two equations for Σ and H (and T) which is obtained by first inserting ν from (37) into (30) and then repeating by inserting ν from (46) to the (30) and then solving these two equations for H :

$$H = \frac{4F^+}{3a\alpha T^4 \Omega} - \frac{c\mathcal{R}T}{F^+ \kappa}. \quad (47)$$

We now can use (41), (40) with (44), (45), (46), and (47) and after much algebra we obtain an equation for T :

$$4(F^+)^2 \kappa \left(6a\alpha c^2 \mathcal{R} T^5 \Omega^2 + (F^+)^2 \kappa (3a\alpha \kappa T^4 - 4c\Omega) \right) - 9a^2 \alpha^2 c^3 \mathcal{R}^2 T^{10} \Omega^3 = 0. \quad (48)$$

Equation (48) can be further simplified down to an equivalently rather compact form:

$$\left(1 - \frac{3a\alpha c \mathcal{R} \Omega}{4(F^+)^2 \kappa} T^5 \right)^2 - \frac{3a\alpha \kappa}{4c\Omega} T^4 = 0. \quad (49)$$

Thus the solution for the disk temperature should be calculated from the non-linear algebraic equation (49). It can be shown that if radiation pressure is neglected, term in the brackets in (49) is left and the corresponding expression for gas pressure alpha disk is recovered:

$$T_c(P_g) = \frac{(3\kappa)^{1/5}(\dot{M})^{2/5}\Omega^{3/5}}{2^{4/5}\pi^{2/5}(\alpha acR)^{1/5}}, \quad (50)$$

from which, for example, the numerical scaling (20) can be calculated.

4.3. Numerical solution

At a given r , with F^+ calculated from (34) and with κ from (51) and Ω from (15), equation (49) is solved numerically. However, some tricks are required to ensure numerical stability. First we assume that above T_{sub} the opacity switches from $\kappa_d + \kappa_e$ to κ_e and approximate $\kappa(T)$ by a bridging formula:

$$\kappa(T) = \frac{\kappa_d}{\exp\left(\frac{T-T_{\text{sub}}}{\Delta T}\right) + 1} + \kappa_e, \quad (51)$$

where the bridging parameter ΔT is fixed at $\Delta T = 0.1$ as well as $\kappa_d = 10 \text{ cm}^2 \text{ g}^{-1}$. Then, to find roots of equation (49) the following procedure is adopted: initial approximation for T_0 is found after $\kappa(T_0)$ is initially estimated from (51), where T_0 obtained for the gas-pressure only solution (20). Then T_0 is used as initial guess to numerically solve (49) with (51) for the true value of T . Finally, multiple roots of equation (49) should be weeded out via checking that they produce positive right-hand-side in the equation (44).

Once T is known the surface density Σ is found from equations (30),(41) and (27), and (40):

$$\Sigma = \frac{64\pi\sigma}{9\kappa} \frac{T^4}{\dot{M}\Omega^2}. \quad (52)$$

The result of a numerical solution of the equation (49) with respect to T is shown in Figure (3) where disk model for $P = P_g$ is compared with the model for $P = P_g + P_r$.

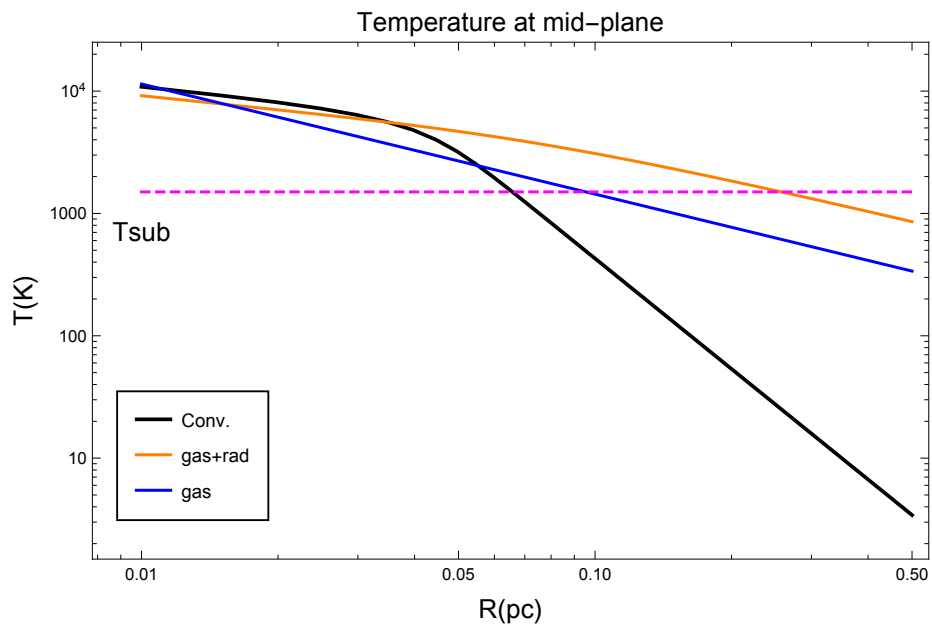


Fig. 3.— Disk temperature at the disk mid-plane. Black: convective. Blue: gas+radiation pressure, equation (49). Orange: gas-pressure-only, equation (20). The intersection with the dashed line, $T_{\text{sub}} = 1500\text{K}$ marks the position of R_{out} .

While this figure more accurately illustrates the relation between R_{in} and R_{out} , we still probably underestimate R_{out} because κ_d becomes important before T is approaching T_{sub} . Thus, the region where the dust opacity changes the vertical structure of the disk is extended further away. From (21) and (22) one can see that the size of this region relatively weakly depends on \dot{M} . Solving equation (49) for different values of parameters, we calculate the size of the active region, i.e. R_{in} and R_{out} . Table 1 summarizes the results for the dependence of R_{in} and R_{out} on \dot{M}_{loc} and column for M_{BH} . Each pair is shown at the intersection of the corresponding row for \dot{M}_{loc} and column for M_{BH} .

$\frac{\dot{M}_{\text{loc}}}{M_{\odot}\text{yr}^{-1}}$ \diagdown $\frac{M_{\text{BH}}}{M_{\odot}}$	10^5	10^6	10^7	10^8	10^9
0.01	5.53×10^{-3}	7.29×10^{-3}	8.61×10^{-3}	9.57×10^{-3}	1.96×10^{-2}
0.01	1.09×10^{-2}	1.81×10^{-2}	7.17×10^{-2}	1.54×10^{-1}	3.33×10^{-1}
0.1	7.29×10^{-3}	8.61×10^{-3}	9.57×10^{-3}	1.02×10^{-2}	2.04×10^{-2}
0.1	4.15×10^{-2}	8.94×10^{-2}	1.93×10^{-1}	4.15×10^{-1}	8.94×10^{-1}
1	8.61×10^{-3}	9.57×10^{-3}	1.02×10^{-2}	2.25×10^{-2}	4.83×10^{-2}
1	1.06×10^{-1}	2.28×10^{-1}	4.9×10^{-1}	1.06	2.28
2	1.72×10^{-2}	9.79×10^{-3}	1.04×10^{-2}	2.84×10^{-2}	6.18×10^{-2}
2	1.37×10^{-1}	2.94×10^{-1}	6.34×10^{-1}	1.36	2.91
10	9.57×10^{-3}	1.02×10^{-2}	2.25×10^{-2}	4.91×10^{-2}	1.06×10^{-1}
10	2.21×10^{-1}	4.76×10^{-1}	1.03	1.86	3.83

Table 1: R_{in} and R_{out} calculated from the numerical solution of equation (49). Left column: accretion rate, \dot{M}_{loc} . Upper row: mass of the Black Hole, M_{BH} . Each cell not belonging to the first row or the first column contains two numbers: upper number: R_{in} ; lower number: R_{out} .

5. Convection

If a gas element which is rising over a small distance, adiabatically and in pressure equilibrium with the environment, is found to be lighter when contrasted to its surroundings, then buoyancy force will keep propelling it further (Kippenhahn & Weigert 1994). The opposite situation corresponds to the Schwarzschild criterion for convective stability:

$$\left| \frac{dT}{dz} \right|_{\text{ad}} > \left| \frac{dT}{dz} \right|. \quad (53)$$

Where $\left(\frac{dT}{dz}\right)_{\text{ad}}$ is the adiabatic and $\frac{dT}{dz} = \left(\frac{dT}{dz}\right)_{\text{rad}}$ radiative temperature gradients (both negative). In this section we revisit assumptions about vertical transport of energy in the disk and show, that as soon as the mid-plane temperature exceeds the sublimation temperature, $T \sim T_{\text{sub}}$, there is a certain range of radii between R_{in} and R_{out} , where the disk is convectively unstable. There are two reasons for convection: 1) As we will show the regular Schwarzschild criterion for the radiative disk indicates that in a wide range of parameters transferring energy vertically by convection is preferred over radiation diffusion. 2) Strong temperature-dependence of the opacity of dust leads to a sudden increase of the radiation pressure at some height above the midplane.

The first point is analogous to convective instability of a radiation-dominated part of a standard α -disk. In a disk in radiative equilibrium, the entropy, S_r , falls abruptly with increasing z and convection drives the equilibrium towards an isentropic state: $S_r \propto \text{const.}$ (Bisnovatyi-Kogan & Blinnikov 1977), where S_r is the entropy of the gas of radiation when $P_r \gg P_g$:

$$S_r = \frac{4}{3} \frac{aT^3}{\rho}. \quad (54)$$

The second point follows from that in a disk in radiative equilibrium $T(z)$ decreases

from the mid-plane (cleared from dust at $T > T_{\text{sub}}$) towards higher z . A dramatic increase of the radiation pressure associated with an opacity jump follows. As long as $T_c > T_{\text{sub}}$, there exists $z_s(r)$ within a vertical column of the disk where there is a transition from dust-free opacity, κ_m to dust opacity, κ_d . Correspondingly $|dT/dz|$ becomes very large at z_s , triggering convection, which works towards smoothing the vertical distribution of the entropy.

The convection establishes a new distribution of ρ and T so as to decrease $|dT/dz|$. Our simplified model discussed so far adopts vertically averaged quantities and a more elaborate treatment of convection calls for more sophisticated methods. The latter is beyond the scope of this paper and in our derivation we estimate the efficiency of convection adopting the solution for the disk in radiative equilibrium as an initial condition.

5.1. Convective region

Our adopted fiducial set of parameters include $R = 0.1$ pc, $T_c = T_{\text{sub}} = 1500\text{K}$ i.e. corresponding to the situation of the dust at exactly the dust sublimation temperature at the disk mid-plane. Estimating dT/dz for $n = 1.84 \times 10^{11} T_{1500}^3 \text{ cm}^{-3}$ corresponding to $P_g = P_r$ case (9), we have

$$\frac{dT}{dz} \propto \frac{T_s - T_c}{H} \simeq -2.7 \times 10^{-12} \text{ K} \cdot \text{cm}^{-1}, \quad (55)$$

where T_s and $T_c = T(z = 0)$ are estimated from the disk model. This should be compared with the adiabatic gradient $\left(\frac{dT}{dz}\right)_{\text{ad}}$ estimated from:

$$\begin{aligned} \left(\frac{dT}{dz}\right)_{\text{ad}} &= -g_z \rho \left(\frac{\partial T}{\partial P}\right)_s = -g_z \rho H \\ &\simeq -1.3 \times 10^{-12} \text{ K} \cdot \text{cm}^{-1}, \end{aligned} \quad (56)$$

where the disk height H is calculated taking into account the equation of state (27). The above estimations are too crude to adopt them in a judgement on convective instability, however from (55) and (56) it follows that in the region of $R_{\text{in}} \lesssim r \lesssim R_{\text{out}}$ adiabatic $\left(\frac{dT}{dz}\right)_{\text{ad}}$ can have similar magnitude as $\frac{dT}{dz}$ warranting further investigation.

For the mixture of gas and radiation, the convective flux is (Kippenhahn & Weigert 1994; Bisnovatyi-Kogan 2001):

$$F_{\text{conv}} = \frac{1}{4} l^2 \rho C_p \left(\frac{g_z}{T}\right)^{1/2} (\Delta\nabla T)^{3/2} \sqrt{\frac{4P_r}{P_g} + 1}, \quad (57)$$

where l is the mixing length, C_p is the heat capacity at constant pressure for the mixture of gas and radiation:

$$C_p = \mathcal{R} \left(\left(\frac{4P_r}{P_g}\right)^2 + \frac{20P_r}{P_g} + \frac{5}{2} \right). \quad (58)$$

The temperature excess of the convective element over its surroundings is represented by $(\Delta\nabla T)$ which is found from:

$$\Delta\nabla T = \left(\frac{\partial T}{\partial P}\right)_s \frac{dP}{dz} - \frac{dT}{dz} = -g_z \rho \left(\frac{\partial T}{\partial P}\right)_s - \frac{dT}{dz}. \quad (59)$$

We adopt $l \simeq \epsilon_0 H$ for the mixing length, where H is the half-thickness of the disk and $\epsilon_0 \leq 1$ is the mixing length parameter for which we adopt the value $\epsilon_0 = 0.1$. Adopting T and ρ from the disk model from Section (4.2), we numerically calculate F_{conv} from (57) and (59). The result is shown in Figure 4, where non-dimensional $\left(\frac{dT}{dz}\right)_{\text{ad}}$ and $\left(\frac{dT}{dz}\right)$ are plotted. Consider the situation when r is decreasing (i.e. tracing the diagram from right-to-left): the curves cross when $\left(\frac{dT}{dz}\right)_{\text{ad}} > \frac{dT}{dz}$ and the medium becomes convectively unstable. In the left column the effect of accretion rate is shown: for $\dot{M}_{\text{loc}} = 0.1 M_{\odot} \text{yr}^{-1}$ the ADR is convective

at $R_{\text{in}} < r < 0.13\text{pc}$; increasing the accretion rate pushes the convective region further out: for $\dot{M}_{\text{loc}} = 2 M_{\odot}\text{yr}^{-1}$, the convective region is at $R_{\text{in}} < r < 0.3\text{pc}$. In the right column one can see a similar effect if the mass of the BH is increased to $M_{\text{BH}} = 10^9 M_{\odot}$.

6. Effects of external irradiation

In presence of illumination by the radiation flux, boundary condition for the surface temperature of the disk, T_s should be modified:

$$\sigma_{\text{B}}T_s^4 = F^+ + f(1 - A)F_n, \quad (60)$$

where F_n is the component of the external flux normal to the surface of the disk, A is the disk albedo, f the attenuation and angular-dependent factor and F^+ is found from (34). Solving radiation transfer equation (36) with (60) we have

$$\sigma_{\text{B}}T^4 = \frac{3}{4}\left(\tau + \frac{2}{3}\right)F^+ + F_{\text{ext}}, \quad (61)$$

where $F_{\text{ext}} = f(1 - A)F_n$ and the photosphere is placed at $\tau = 2/3$. From (61) one can see that if $F^+\tau_c \gg F_n$, the mid-plane temperature, T_c is practically independent from external sources of heating (Lyutiy & Sunyaev 1976). The total attenuation factor in (60) is approximately $0.5e^{-2/3} \simeq 1/4$ for $A \simeq 0.5$.

Vertical structure of the disk is calculated from (32), and (36), yielding vertical distribution of temperature in the illuminated disk:

$$T = T_c \left(1 - \frac{3}{2} \frac{\tau_c F^+}{T_c^4} \left(\frac{\sigma}{\sigma_c} \right)^2 \right), \quad (62)$$

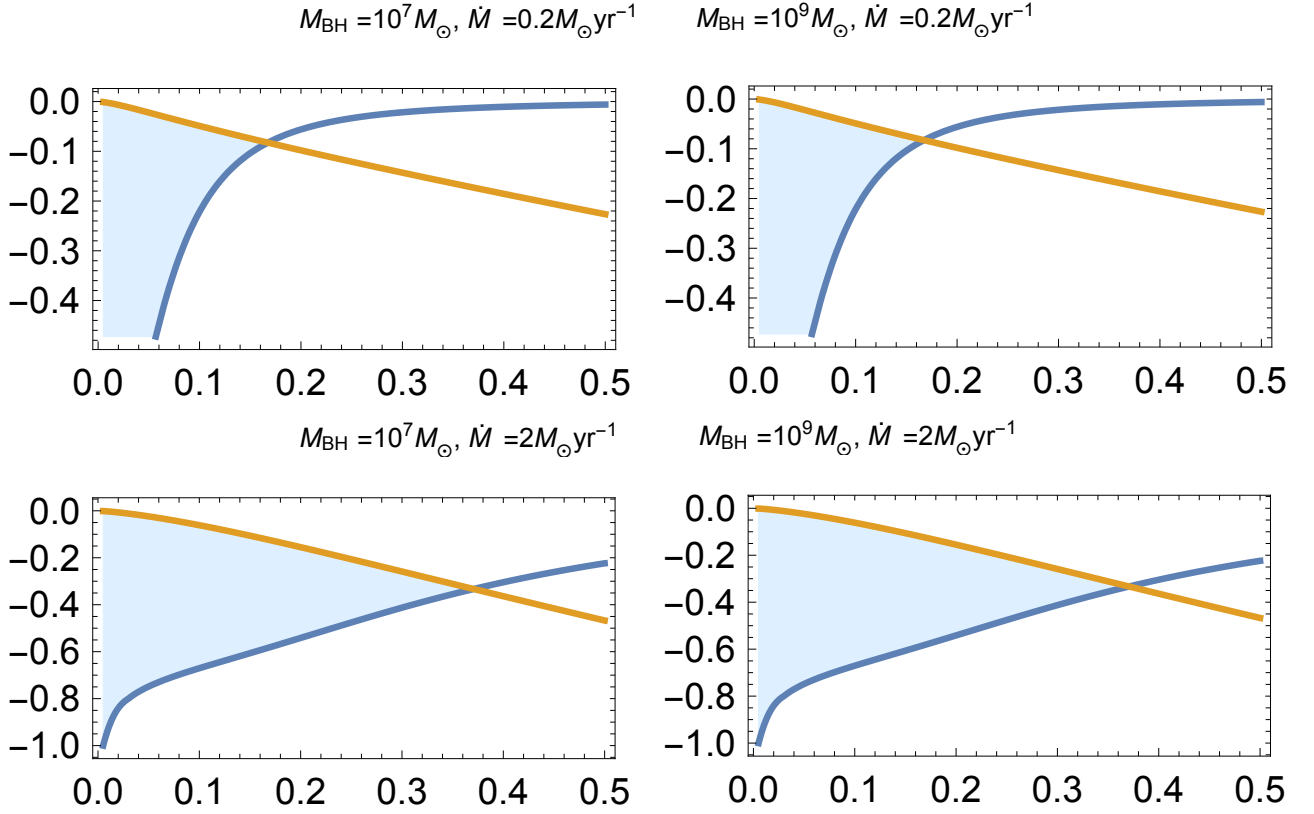


Fig. 4.— Transition to convection at the disk mid-plane. Shown are non-dimensional (in code units) gradients: $(\frac{dT}{dz})_{\text{ad}}$ -orange line; actual $\frac{dT}{dz}$ - blue line. Horizontal axis: distance from the BH in pc. Shaded area: region of convective instability.

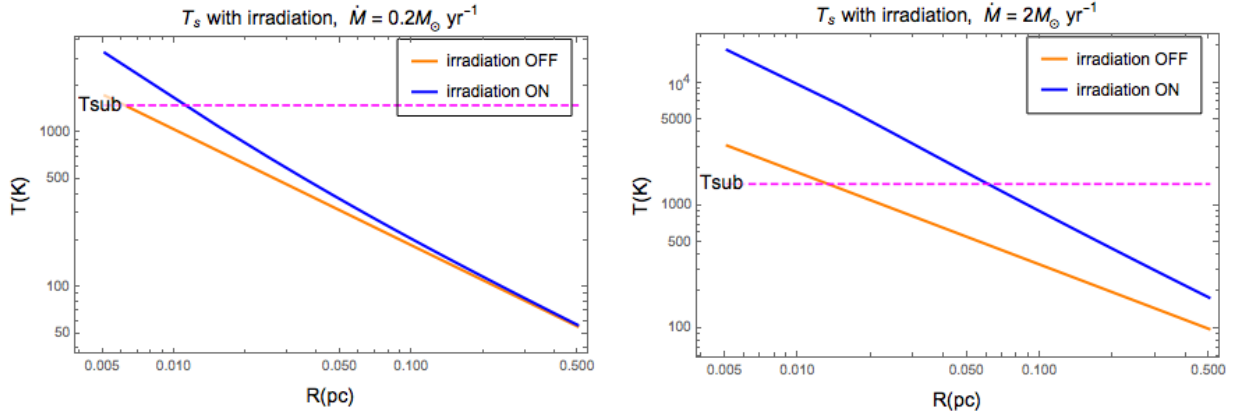


Fig. 5.— Effect of the illumination on the surface temperature of the disk.

where we assumed the specific rate of viscous energy dissipation to be constant, $\tau_c \simeq \sigma_c \kappa_d$. Surface temperature as found from (60) can, on the other hand, be significantly influenced by the external radiation flux:

$$F_{\text{ext}} \simeq \delta(1 - A) \frac{L}{4\pi r^2} \mu(2\mu + 1), \quad (63)$$

where L is calculated from (1) and the factor $\delta \simeq H/r$ is related to the angle between the surface of the disk and the direction of radiation flux (Meyer & Meyer-Hofmeister 1982; Spruit 1996). Estimating δ from (16):

$$\delta \simeq \frac{3}{8\pi} \frac{\kappa_d}{cR} \dot{M}. \quad (64)$$

The effect from the external flux is demonstrated in Figure 5 which shows T_c and T_s for $A = 0.5$. Not surprisingly, T_s is noticeably influenced by irradiation.

In case of the central radiation flux, the dominating component of radiation force is directed very nearly along the disk surface. The vertical radiation pressure in a single-scattering

approximation, scales in the same way as the gravitational force. Thus illumination of a thin disk by the UV flux is unlikely responsible for "puffing up" of the AGN disk at pc-scales. X-rays penetrate much deeper, and can potentially lead to a much stronger "puffing up" due to IR pressure (Chang et al. 2007; Dorodnitsyn et al. 2016).

The predictive power of our simple calculations of the effect of the irradiation is limited. The attenuation of the radiation flux from the nucleus depends on the obscuring properties of winds at smaller radii and can be addressed only via global numerical modeling.

6.1. Dust above the disk

Dust above the disk at $R < R_{\text{sub}}$ is exposed to the weathering UV and X-ray illumination from the nucleus. In general, the gas-dust medium is a very efficient UV absorber. The unattenuated UV radiation is promptly stopped in a very thin layer where it is further converted into IR as well as heating the gas. The UV opacity of the $0.1\mu\text{m}$ grain is about its geometrical cross-section, $\kappa_{\text{UV}} \simeq 10^2 f_{\text{d},0.01} \text{cm}^2 \text{g}^{-1}$, where $f_{\text{d},0.01}$ is gas to dust mass ration in 10^{-2} . The thickness of such a "photospheric" layer is

$$\delta l_{\text{UV}}/r_{\text{sub}}^{\text{UV}} \simeq 5 \times 10^{-2} f_{\text{d},0.01} n_5^{-1} L_{46}^{-1/2}, \quad (65)$$

while the penetration length of X-rays is significantly higher:

$$\delta l_{\text{XR}}/r_{\text{sub}}^{\text{UV}} \simeq \begin{cases} 0.023, & 0.5 < E < 7\text{keV} \\ 0.014, & E > 7\text{keV} \end{cases} \times n_5^{-1} L_{46}^{-1/2}, \quad (66)$$

where κ_{XR} is the X-ray opacity consisting of photoionization and Compton cross sections. In general $\delta l_{\text{XR}} \simeq \frac{\kappa_{\text{UV}}}{\kappa_{\text{XR}}} \delta l_{\text{UV}}$. We adopt the photo-ionization cross-section from (Maloney et al. 1996): for $0.5 < E < 7$ keV we have $\sigma_{\text{XR}} \simeq 2.6 \times 10^{-22} \text{cm}^2$ and for $E > 7\text{keV}$: $\sigma_{\text{XR}} \simeq$

$4.4 \times 10^{-22} \text{cm}^2$.

Within the UV conversion layer the UV radiation exerts pressure of the order of $P_r \simeq 0.03 \text{ dyn cm}^{-2}$ on the dusty surface of the disk/torus. If, from within the disk, such a layer is supported entirely by the gas pressure, then, recalling that the equilibrium density at $P_r = P_g$, is $n \simeq 10^{11} \text{ cm}^{-3}$ (9), the UV penetration length can be estimated to be just $10^{-8} - 10^{-7} r_{\text{sub}}^{\text{UV}}$.

Illumination by an X-ray flux has a devastating effect on the dust in an optically thin region. The sudden exposure of the gas-dust slab would create a receding evaporation layer where gas is transitioning from cold to $10^4 - 10^6 \text{ K}$ hot component (i.e. Dorodnitsyn et al. 2008). It is not until such an X-ray flux is sufficiently (i.e. $\tau_{\text{xw}} \simeq 1$) attenuated in the X-ray evaporative gas/wind, when enough dust can survive, and the UV conversion layer has a chance to actually settle.

The opacity of gas-dust mixture in the UV and IR is dominated by the opacity of dust, κ_d , with two major contributors: silicon at lower, and carbon at higher temperatures. Such temperature dependence can be approximately described as

$$\kappa_d = \kappa_0 \left(\frac{T}{T_{\text{sub}}} \right)^n \quad \text{for } T < T_{\text{sub}}, \quad (67)$$

where $\kappa_0 = 10 - 50 \text{ cm}^2 \text{ g}^{-1}$ (Semenov et al. 2003), and $n \simeq 1 - 2$, when $T_g \gg T_s$. In general, dust grain sublimation time-scale, t_{sub} is very short. The mass of the dust grain can increase or decrease depending on $\Delta P = p_{\text{vap}} - p_i$, where p_{vap} is the saturation vapor pressure, and p_i is the partial pressure of the specie, i (Phinney 1989). The dust grain sublimation time-scale can be estimated as

$$t_{\text{sub}} = \frac{m_{\text{gr}}}{\dot{m}_{\text{gr}}}, \quad (68)$$

where m_{gr} is the mass of a dust grain, $\dot{m}_{\text{gr}} = 4\pi a^2 P_{\text{vap}} \sqrt{\frac{\mu_i m}{2\pi k T}}$ is the dust grain mass-loss rate density, μ_i is the molecular weight, and m_u is the atomic mass unit. Since $P_{\text{vap}} \sim \exp(-\text{few} \cdot 10^4/T)$ it is a very sensitive function of the gas temperature. Corresponding time-scale is very short compared to t_{th} , t_{dyn} . For example, evaluating (68) for amorphous silicon dust, it is just

$$t_{\text{sub}}(\text{MgFeSiO}_4) \simeq 0.22 \text{ days}, \quad (69)$$

and $t_{\text{sub}} \ll t_{\text{dyn}}, t_{\text{th}}$ indeed follows.

7. Discussion

It has been suggested by (Czerny & Hryniewicz 2011) that the pressure of the disk's own, local radiation on dust can drive large-scale "failed" winds. Baskin & Laor (2018) recalculated the dust opacity based on the inclusion of the new data for graphite grains. The same authors predicted in that in result of such enhanced opacity, such a disk can "bulge up" and form a compact torus at approximately $\text{few} \times 10^{-2} \text{pc}$. In this work we focus on a generally much broader region where radiation pressure can impact the vertical structure of the accretion disk in AGN. As the dusty gas spirals from galactic scales towards the nucleus it is generally quite cold so that the disk is very thin. Closer to the BH gas heats up due to internal viscous dissipation until such internally generated radiation starts to influence the vertical structure of the disk via radiation pressure on dust grains.

The disc mid-plane temperature increases towards smaller r as $T_c \propto r^{-9/10} \simeq r^{-1}$. At the radius R_{out} the mid-plane temperature, T_c equals the temperature of dust sublimation $T_{\text{sub}} \simeq 1500 \text{K}$. Already when T_c reaches several hundred K, the contribution from radiation pressure on dust increases. When $T_c > T_{\text{sub}}$ the mid-plane is cleared from dust and the total

pressure at the mid-plane is dominated by that of the gas. However just above the mid-plane as the temperature drops to $T(z) < T_{\text{sub}}$ opacity increases by approximately two orders of magnitude and so does the coupling between vertical radiation flux and the dusty gas. AGN accretion disks thus have two regions where radiation pressure is important: one close to the BH as predicted by the standard SS73 theory, and the other considerably further away, approximately at $R_{\text{in}}(T_s = T_{\text{sub}}) < R < R_{\text{out}}(T_c = T_{\text{sub}})$.

The mass accretion rate in ADR (ADR) does not need to correspond to the mass accretion rate derived from the bolometric luminosity of the nucleus, $L \propto \dot{M}$ where \dot{M} is the accretion rate within inner parts of the accretion disk. The latter is approximately limited by the Eddington accretion rate: $\dot{M}_{\text{E}} \simeq 0.2M_7 M_{\odot}\text{yr}^{-1}$. The *local* production rate of radiation in a disk depends on the local mass-accretion rate, \dot{M}_{loc} . Correspondingly, for the envelope of a disk to "puff up" and become slim such disk should have the local mass-accretion rate, $\dot{M}_{\text{loc}} > \dot{M}_{\text{loc,cr}}$, where $\dot{M}_{\text{loc,cr}}$ is the Eddington mass-accretion rate as calculated with respect to the opacity of dust. Depending on assumptions about dust, $\dot{M}_{\text{loc,cr}} \simeq 2.4 - 10 M_{\odot}\text{yr}^{-1}$. If \dot{M}_{loc} in ADR is larger than \dot{M} the excess gas should be removed by the winds, or participate in large-scale flows.

In this paper we necessarily made many simplifications. For example, when establishing that ADR disk is highly convectively unstable we did not quantitatively address the problem that the vertical structure of such a disk should be considerably altered by convection. Instead, we assumed that in the convective layer the convection is so efficient that it drives the equation of state to an isentropic one. In reality we expect the total vertical flux of energy to have contributions from both convection and from radiation. We notice though, that due to the very large dust opacity we expect our main conclusions to stand: ADR is expected to be convective for a wide range of parameters.

When considering disk irradiation and its influence on the disk structure we only con-

sidered how such illumination changes the surface boundary condition for the radiation transfer problem. Such a quasi-1D approach gives qualitatively correct results but more detailed treatment should include angular dependent effects which can be important when disk becomes geometrically thick.

Analogies between accretion disk physics and outflowing stellar atmospheres can be helpful. The case of a luminous star atmosphere with high radiation pressure in continuum, in a regime in which the convection solution competes with the outflowing one was calculated in (Bisnovatyi-Kogan 1973). It was found that the increase of the radiation flux (in our case the equivalent to the increase of \dot{M}_{loc}) leads there to the transition from convective solution to an outflowing one with some overlap between the two. In this paper we did not calculate such outflowing solutions, but the stellar analogy provides some evidence that such a transition may happen. Detailed calculations in disk geometry are significantly more difficult, at a very minimum requiring multi-dimensional numerical simulations.

After the dusty gas is expelled from the disk it is exposed to radiation pressure forces from the nucleus which can be significantly greater than the vertical radiation pressure from the disk itself. Depending on \dot{M} and \dot{M}_{loc} different types of dusty outflows can be envisaged: from thin layered flows along the disk surface, to the large-scale, but gravitationally bound "failed winds", to polar hollow cone dusty outflows of different curvature. Example of such a wind is shown in Figure 2.

To produce massive outflow most efficiently two factors should align: the local accretion rate should be greater than the local critical rate, $\dot{M}_{\text{loc}} > \dot{M}_{\text{loc,cr}}$ and the location of ADR should be such as $R_{\text{out}} \gtrsim R_{\text{sub}}$. Self-regulation of accretion due to the disk's own radiation pressure on dust can be important for the regulation of the SMBH growth through accretion and deserves further investigation.

8. Conclusions

Our results can be summarized as follows:

- We have shown that there is a region in an AGN accretion disk in which local radiation pressure on dust can have a major effect on the disk vertical structure and dynamics.
- Such an Active Dusty Region (ADR) is approximately bounded at large radius by the dust sublimation radius on the disk mid-plane and at small radius by the dust sublimation radius at the disk surface.
- The outer boundary of ADR in the disk is approximately identified as the radius, R_{out} where the temperature at the disk mid-plane equals the dust sublimation temperature, T_{sub} . For $M_{\text{BH}} = 10^7 M_{\odot}$, $R_{\text{out}} \simeq 0.1 \text{pc}$. At $R < R_{\text{out}}$ dust is cleared near the mid-plane and there is a dramatic jump of opacity along the vertical through the disk.
- The inner boundary of ADR is located at the radius where dust completely disappears inside the disk, i.e. at $T_s = T_{\text{sub}}$, where T_s is the disk surface temperature.
- We have shown that ADR is strongly convectively unstable with significant vertical energy transport via convection. Convection results in effective cooling of the disk interior. It is also possible that the convection from the ADR provides the turbulence driver for the BLR.

This work was supported by NASA grant 14-ATP14-0022 through the Astrophysics Theory Program.

Appendix: Convective disk

When energy is transported towards the surface of a disk via convection it is often the case that $F_{\text{conv}} \gg F_{\text{rad}}$ where F_{conv} and F_{rad} are convective and radiation fluxes respectively. Convection tends to establish isentropic distribution: $S = \text{const.}$ where S is found from (54). Thus, to describe fully convective disk one adopts polytropic equation of state for radiation Bisnovatyi-Kogan & Blinnikov (1977):

$$P = K\rho^{4/3}, \quad (70)$$

where

$$K = \left(\frac{3S^4}{256a} \right)^{1/3} \simeq \text{const.} \quad (71)$$

Inserting polytropic e.s. (70) equation (42) gives:

$$\frac{dP}{dz} = -\Omega^2 K^{-3/4} z P^{3/4}. \quad (72)$$

Solving further this equation, one can eventually obtain the following simple relations:

$$\rho \simeq \rho_c \left(1 - \frac{z^2}{z_b^2} \right)^3, \quad (73)$$

$$P \simeq P_c \left(1 - \frac{z^2}{z_b^2} \right)^4, \quad (74)$$

When simplifying (73),(74) we took into account that $P_b \ll P_c$, $\rho_b \ll \rho_c$ and adopting *these relations* for simplicity the assumptions: $P_b \simeq 0$, $\rho_b \simeq 0$ at $z = z_b$, where ρ_b and P_b are the corresponding values at the boundary of the disk. A surface boundary condition follows from integrating (13) between z_b and infinity: $P_b = z_b \Omega^2 \tau_b / \kappa_d$, where $\tau_b \simeq 2/3$, and

all properties of a polytropic disk can then be derived as in (Bisnovatyi-Kogan & Blinnikov 1977).

9. Glossary

Symbol	description, Sec., (eq. number)
ADR	"Active Dusty Region", 1
L	total luminosity, Sec.2.1, (1)
M	mass of the BH, Sec.2.1
ϵ	accretion efficiency, Sec.2.1, (1)
\dot{M}	mass-accretion rate near BH, Sec.2.1, (1)
L_E	Eddington luminosity, Sec.2.1, (2)
κ_e	electron opacity, cm^2g^{-1} , Sec.2.1
R	radius in physical units, Sec.2.1
r	radius in scaled units, Sec.2.1
R_{AGN}	"outer radius of AGN", Sec.2.1, (4)
σ_{Blg}	bulge stellar velocity dispersion, Sec.2.1, (4)
R_g	Schwarzschild radius, Sec.2.1, (5)
Ω	angular velocity in the disk
T	gas temperature, Sec.2.1
ρ	gas density, Sec.2.1
n	gas number density, Sec.2.1
H	thickness of AGN disk, Sec.2.1, (6)
F_{ext}	flux from the nucleus, 2.1, (7)
F_{loc}	disk local radiation flux, Sec.2.1, (8)
F_{tot}	total vertical energy flux in a disk, 7
θ	inclination angle from the normal to the disk, Sec.2.1
μ	$\cos \theta$, Sec.2.1, (7)
$f(\theta)$	angular dependence of the radiation flux, Sec.2.1, (7)
\dot{M}_{loc}	local mass-accretion rate near BH, Sec.2.1, (8)

\mathbf{g}_{rad}	radiation pressure vector, Sec.2.1
n_{eq}	density at which $P_g = P_r$, Sec.2.1, (9)
P_g	gas pressure, Sec.2.1, (10)
\mathcal{R}_{gas}	gas constant, Sec.2.1
μ_m	mean molecular weight, Sec.2.1, (10)
\mathcal{R}	\mathcal{R}/μ_m -modified gas constant, Sec.2.1
P_r	radiation pressure, Sec.2.1, (11)
a	radiation constant, Sec.2.1, (11)
t_{dyn}	free-fall time-scale, Sec.2.1
v_r	radial velocity, Sec.2.1
α	viscosity parameter, Sec.2.1
t_a	disk accretion time-scale, Sec.2.1, (12)
t_{visc}	disk viscous time-scale, Sec.2.1, (12)
t_{th}	disk thermal time-scale, Sec.2.1
κ	opacity of the accreting material, Sec.2.2, (13)
κ_d	dust opacity, Sec.2.2, (67)
κ_{UV}	UV dust opacity, Sec.6.1
κ_{XR}	X-ray gas opacity, Sec.6.1
σ_{XR}	X-ray gas cross-section opacity, Sec.6.1
g_z	vertical gravitational acceleration, Sec.2.2, (14)
Ω_K	Keplerian angular velocity, Sec.2.2, (15)
$\dot{M}_{\text{loc,cr}}$	Eddington accretion rate for dust opacity, Sec.2.2, (17)
$T_{\text{vir,r}}$	“virial” temperature for the radiation dominated medium, Sec.2.2, (18)
T_s	temperature at the disk surface, Sec.3, (19)
T_c	mid-plane temperature, Sec.3, (20)
Σ_c	disk surface density, Sec.3

τ_c	mid-plane optical depth of the disk, 3
τ_{phot}	optical depth at the disk photosphere, Sec.3
σ_B	Stefan-Boltzmann constant, Sec.3
R_{in}	inner dust sublimation radius in the disk Sec.3, (21)
R_{out}	outer dust sublimation radius in the disk Sec.3, (22)
R_{sub}	global dust sublimation radius Sec.3, (25)
P	total pressure Sec.4, (27)
Σ	surface density, Sec.4, (29)
F	vertical radiation flux, Sec.4, (32)
F^+	vertical radiation flux from the surface , Sec.4, (32)
F_{conv}	convective flux Sec.5, (57)
ν	effective viscosity , Sec.4, (46)
q_v	specific rate of viscous energy dissipation, Sec.4, (33)
σ	mass coordinate , Sec.4 (35)
H_g	scale-height of the equatorial gas layer of the disk, Sec.4.2, (39)
$T_{\text{c,gas}}$	$T_{\text{c,gas}}$
$\left(\frac{dT}{dz}\right)_{\text{ad}}$	adiabatic temperature gradient, Sec.5, (56)
$\left(\frac{dT}{dz}\right)_{\text{rad}}$	radiative temperature gradient, Sec.5, (56)
S_r	entropy of the radiation gas Sec.5, (54)
C_p	heat capacity at constant pressure, Sec.5, (58)
$\Delta\nabla T$	temperature excess of the convective element, Sec.5, (59)
l	mixing length, Sec.5
ϵ_0	mixing length parameter, Sec.5
F_n	component of the external flux normal to the surface of the disk, Sec.6, (60)
A	disk albedo, Sec.6, (60)
δ	angle between the surface of the disk and the direction of radiation flux, Sec.6, (63)

δl_{UV} thickness of the UV conversion layer, Sec.6.1, (65)

δl_{XR} thickness of the X-ray conversion layer, Sec.6.1, (66)

t_{sub} dust grain sublimation time-scale, Sec.6.1, (68)

REFERENCES

Antonucci, R. R. J. 1984, ApJ, 278, 499

Antonucci, R. R. J., & Miller, J. S. 1985, ApJ, 297, 621

Baskin, A., & Laor, A. 2018, MNRAS, 474, 1970

Bisnovatyi-Kogan, G. S. 1973, Ap&SS, 22, 307

—. 2001, Stellar physics. Vol.1: Fundamental concepts and stellar equilibrium

Bisnovatyi-Kogan, G. S., & Blinnikov, S. I. 1977, A&A, 59, 111

Bisnovatyi-Kogan, G. S., & Lovelace, R. V. E. 2000, ApJ, 529, 978

—. 2007, ApJ, 667, L167

Chang, P., Quataert, E., & Murray, N. 2007, ApJ, 662, 94

Czerny, B., & Hryniewicz, K. 2011, A&A, 525, L8

Dorodnitsyn, A., Bisnovatyi-Kogan, G. S., & Kallman, T. 2011, ApJ, 741, 29

Dorodnitsyn, A., Kallman, T., & Proga, D. 2008, ApJ, 687, 97

—. 2016, ApJ, 819, 115

Jaffe, W., et al. 2004, Nature, 429, 47

- Kaspi, S., Smith, P. S., Netzer, H., Maoz, D., Jannuzi, B. T., & Givon, U. 2000, *ApJ*, 533, 631
- Kippenhahn, R., & Weigert, A. 1994, *Stellar Structure and Evolution*, ed. Kippenhahn, R. & Weigert, A.
- Koshida, S., et al. 2014, *ApJ*, 788, 159
- Lovelace, R. V. E., Romanova, M. M., & Biermann, P. L. 1998, *A&A*, 338, 856
- Lubow, S. H., Papaloizou, J. C. B., & Pringle, J. E. 1994, *MNRAS*, 267, 235
- Lynden-Bell, D., & Pringle, J. E. 1974, *MNRAS*, 168, 603
- Lyutiy, V. M., & Sunyaev, R. A. 1976, *Soviet Ast.*, 20, 290
- Maloney, P. R., Hollenbach, D. J., & Tielens, A. G. G. M. 1996, *ApJ*, 466, 561
- Meyer, F., & Meyer-Hofmeister, E. 1982, *A&A*, 106, 34
- Murray, N., Quataert, E., & Thompson, T. A. 2005, *ApJ*, 618, 569
- Peterson, B. M., et al. 2004, *ApJ*, 613, 682
- Phinney, E. S. 1989, in *NATO ASIC Proc. 290: Theory of Accretion Disks*, ed. F. Meyer, 457–+
- Proga, D., & Kallman, T. R. 2004, *ApJ*, 616, 688
- Raban, D., Jaffe, W., Röttgering, H., Meisenheimer, K., & Tristram, K. R. W. 2009, *MNRAS*, 394, 1325
- Rowan-Robinson, M. 1977, *ApJ*, 213, 635
- Semenov, D., Henning, T., Helling, C., Ilgner, M., & Sedlmayr, E. 2003, *A&A*, 410, 611

- Shakura, N. I. 1972, *AZh*, 49, 921
- Shakura, N. I., & Sunyaev, R. A. 1973, *A&A*, 24, 337
- Sobolev, V. V. 1975, *Course of theoretical astrophysics*.
- Spruit, H. C. 1996, in *NATO Advanced Science Institutes (ASI) Series C*, Vol. 477, NATO Advanced Science Institutes (ASI) Series C, ed. R. A. M. J. Wijers, M. B. Davies, & C. A. Tout, 249–286
- Suganuma, M., et al. 2006, *ApJ*, 639, 46
- Sunyaev, R. A., & Titarchuk, L. G. 1985, *Astronomy and Astrophysics*, 143, 374
- Tristram, K. R. W., Burtscher, L., Jaffe, W., Meisenheimer, K., Hönig, S. F., Kishimoto, M., Schartmann, M., & Weigelt, G. 2014, *A&A*, 563, A82
- Tristram, K. R. W., & Schartmann, M. 2011, *A&A*, 531, A99
- Urry, C. M., & Padovani, P. 1995, *PASP*, 107, 803
- Zhu, Z., & Stone, J. M. 2018, *ApJ*, 857, 34